MOLECULAR AND CELLULAR BIOLOGY, Jan. 1989, p. 336–341
0270-7306/89/010336-06$02.00/0

Vol. 9, No. 1

Electron Microscopy Reveals that Transcription Factor TFIIIA Bends 5S DNA

D. P. BAZETT-JONES* AND M. L. BROWN

Department of Medical Biochemistry, The University of Calgary, 3330 Hospital Drive N.W., Calgary, Alberta T2N 4N1, Canada

Received 28 July 1988/Accepted 11 October 1988

We have used a high-resolution analytical electron microscopic technique, electron spectroscopic imaging, to study the in vitro interaction between the transcription factor IIIA (TFIIIA) and 5S ribosomal gene DNA. The images and analytical measurements support our proposal that the helix axis is bent by the protein into a hairpin-shaped configuration.

A 39,000-molecular-weight (MW) protein called TFIIIA is required along with two other components, TFIIIB and TFIIIC, for accurate initiation of transcription of the 5S ribosomal RNA genes by polymerase III (6, 8, 9, 13). DNase protection assays and deletion mapping show that one molecule of TFIIIA interacts with an internal control region that spans about 50 nucleotides from +49 to +97 within the 5S gene (2, 12, 15). Furthermore, DNase I cutting of DNA bound to TFIIIA is reminiscent of the cutting pattern of nucleosomal DNA or DNA wrapped on a surface, having a 10.4-base-pair (bp) repeat (4, 11). From these studies, it has been proposed that the protein binds to one side of the DNA helix, the zinc finger DNA binding motifs projecting alternately into the major groove on either side of the double helix (3, 7, 11).

Conventional approaches for imaging the interaction of a protein with a molecular weight as low as that of TFIIIA with DNA by staining and shadowing would likely obscure useful structural information. We chose to examine the complex with electron spectroscopic imaging (ESI) because it offers a number of advantages. First, the use of electrons that have lost energy in the low end of the energy loss spectrum provides a dark-field-like image of very high contrast, thereby eliminating the requirement of heavy atom contrast agents. A second advantage of ESI is its ability to generate a phosphorus distribution of a protein-DNA complex (1, 1a) that thereby provides the location of the nucleic acid component.

Preparation of TFIIIA-DNA complexes. 7S ribonucleoprotein particles were isolated from immature oocytes of *Xenopus laevis* as described by Hanas et al. (5). TFIIIA was then purified from the 7S particles by using the protocol described by Smith et al. (15). Complexes of TFIIIA with 5S gene DNA were formed on either the cloned *Xenopus* somatic-type 5S gene (pXP-10) (17) or the oocyte-type 5S DNA (pXlo8) (1b) as described previously (15). The plasmids were digested with a single-cutting restriction enzyme for mapping the complexes. DNA at a concentration of about 800 μg/ml was mixed with purified TFIIIA (Fig. 1) at a ratio of 3 mol of protein to 1 mol of DNA binding site in a buffer containing 10 mM Tris (pH 7.5), 8% glycerol, 4 mM $MgCl_2$, 25 μM $ZnCl_2$ and 1 mM dithiothreitol. After an incubation at 22°C for 15 min, the reaction mixture was filtered on a 2.0 ml Bio-Gel A 5-m column at 4°C.

DNA-protein complexes were diluted to a concentration of 5 μg/ml before a 5-μl drop was immediately applied to a 1,000-mesh grid that had previously been coated with a carbon support film 2 to 3 nm in thickness. After 1 min, the grid was washed with distilled water and air dried. No structural differences were observed if the specimens were dried from distilled water or from either 0.01% glucose solution or a 0.5% Photo-flo (Eastman Kodak Co.) (pH 8.5) solution. ESI was performed on a Zeiss EM902 electron microscope equipped with an imaging prism-mirror-prism-type electron spectrometer (1a).

ESI of TFIIIA-DNA complexes. A low-magnification-field

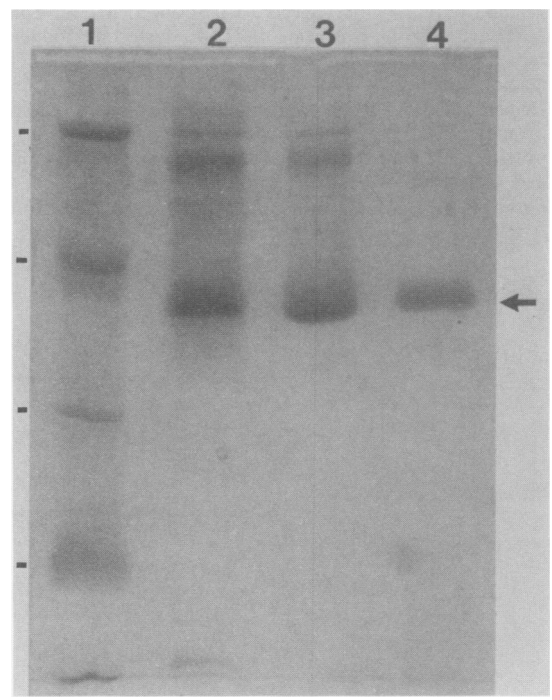

FIG. 1. Sodium dodecyl sulfate-polyacrylamide electrophoresis gel of TFIIIA at various stages of purification. Lanes; 1, MW markers (low MW; BioRad Laboratories); 2, protein present in 7S-containing fractions removed from the glycerol gradient; 3, protein content of the 7S preparation after DEAE-cellulose chromatography; 4, purified TFIIIA after RNase A digestion of 7S particles and ion-exchange chromatography. Protein was visualized by silver staining. Arrow indicates 40,000 MW, and the markers on the left represent 22,000, 31,000, 66,000, and 97,000 MW.

* Corresponding author.

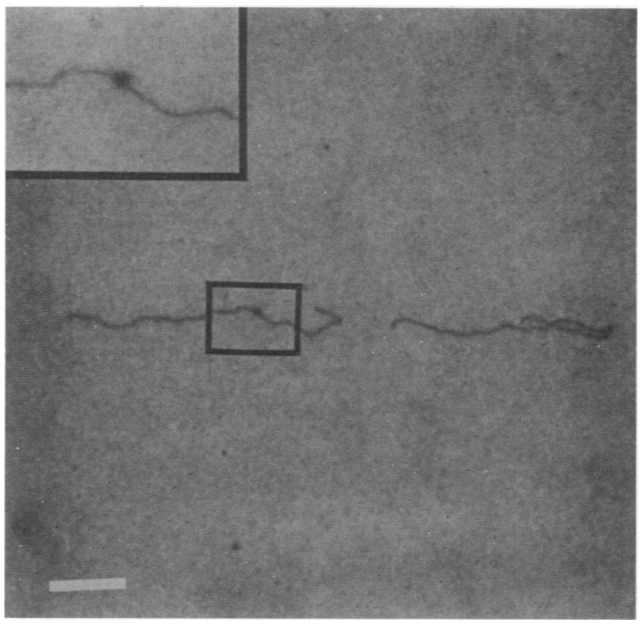

FIG. 2. Low-magnification-field view of two molecules of the plasmid pXb10 digested with *Xmn*I. The DNA was complexed with purified TFIIIA at a ratio at which about 1 of 7 of the DNA molecules contained a protein complex. The image was recorded in the energy loss mode with electrons that had lost 120 eV. The inset is a higher magnification of the indicated region. Bar, 230 nm.

view (Fig. 2) shows two DNA plasmid molecules, the left one containing a single complex with a mass density significantly greater than the linear mass density of DNA itself. The insert is a higher magnification of the indicated area. An input ratio of 3 mol of TFIIIA per mol of 5S gene resulted in the appearance of such a structure on approximately 1 of 7 (33 of 240) DNA strands. Low input ratios were chosen to avoid nonspecific interactions and clumping of the DNA on the grid. The low frequency of objects of similar mass appearing in the background makes us confident that this more massive feature on the DNA represents TFIIIA binding. This was further supported by contour mapping of these complexes on both the somatic- and oocyte-type 5S gene-containing plasmids (Fig. 3).

ESI images recorded at 120 eV energy loss of other TFIIIA-DNA complexes are shown in Fig. 4. The striking feature of the complex is that it appears as a mass with a width from 4 to 6 nm on one side of the DNA helix and extends as much as 11 nm out from the axis of the DNA helix. Measurements from 50 images of these complexes gave an average width of 5.2 ± 0.7 nm, ranging from 4.2 to 6.5 nm, and an average extension from the helix axis of the flanking DNA of 9.4 ± 1.7 nm, ranging from 5.0 to 11.3 nm. Clearly, the projection angle influences the values of these two orthogonally related measurements. Despite the variability in these two dimensions it is quite obvious that the complex does not appear as an increased density extending along the DNA helix for approximately 15 nm, nor does it appear as a 15-nm mass lying alongside the DNA molecule. Such morphology would support the structural model of the interaction proposed by Fairall et al. (3), but such complexes were not found in our micrographs.

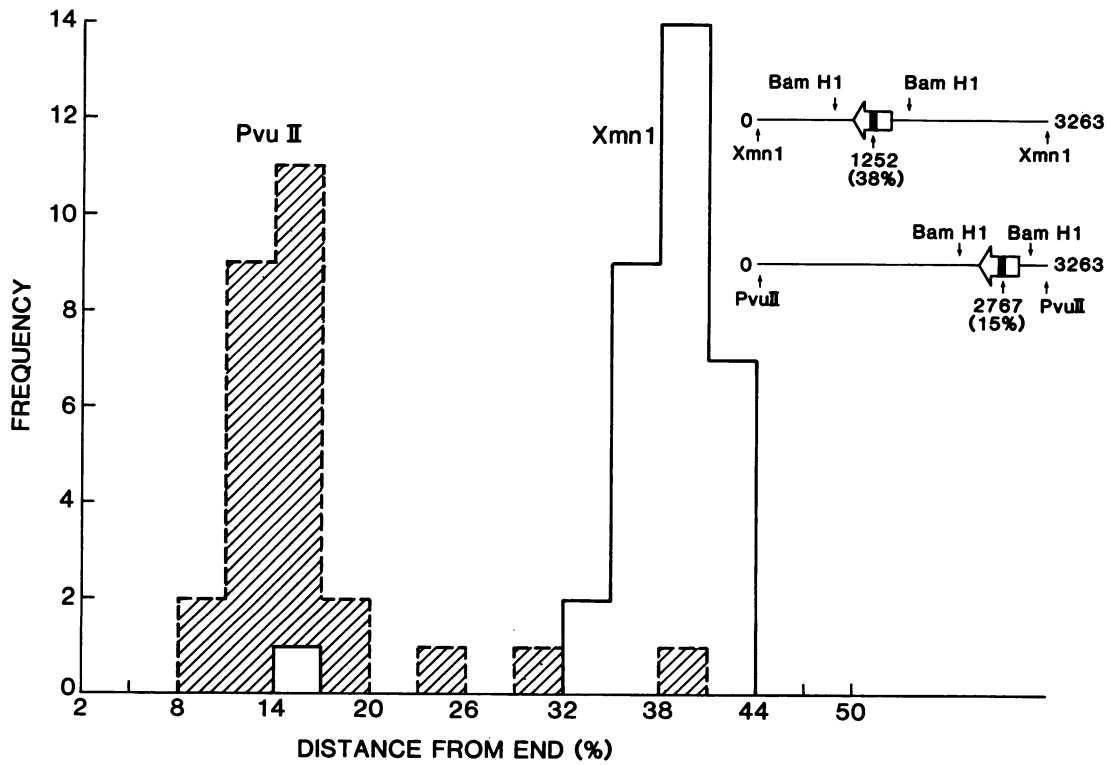

FIG. 3. Protein-DNA complex locations determined by contour mapping on the somatic-type 5S gene-containing plasmid, pXP-10. Two distributions are shown for which the plasmid has been linearized with either *Xmn*I or *Pvu*II. Restriction maps of the plasmid with the expected binding sites are presented at the upper right.

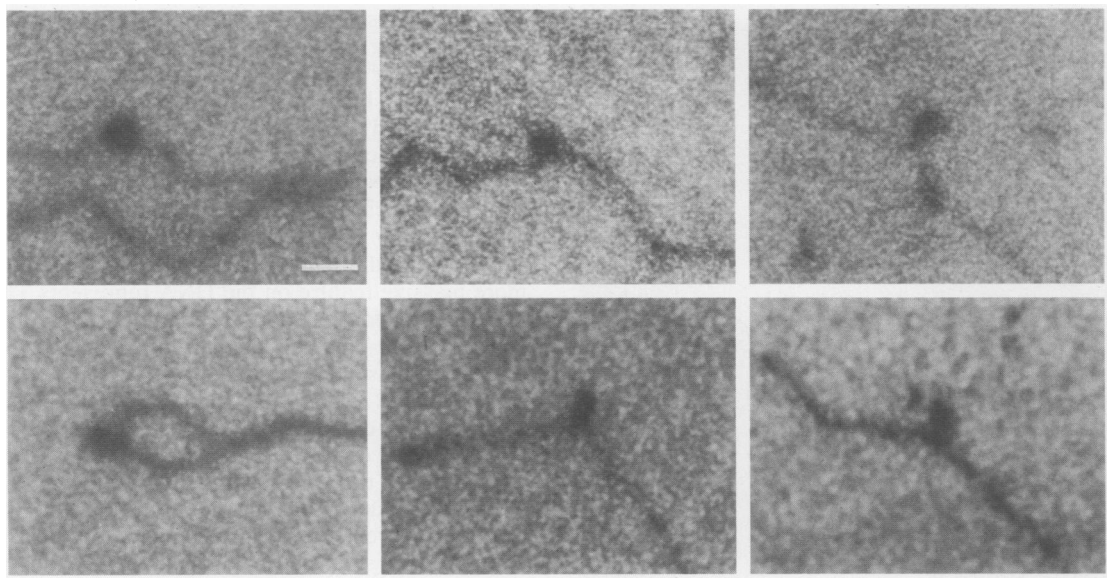

FIG. 4. ESI of TFIIIA-DNA complexes (recorded at 120 eV of energy loss). Bar, 13.8 nm.

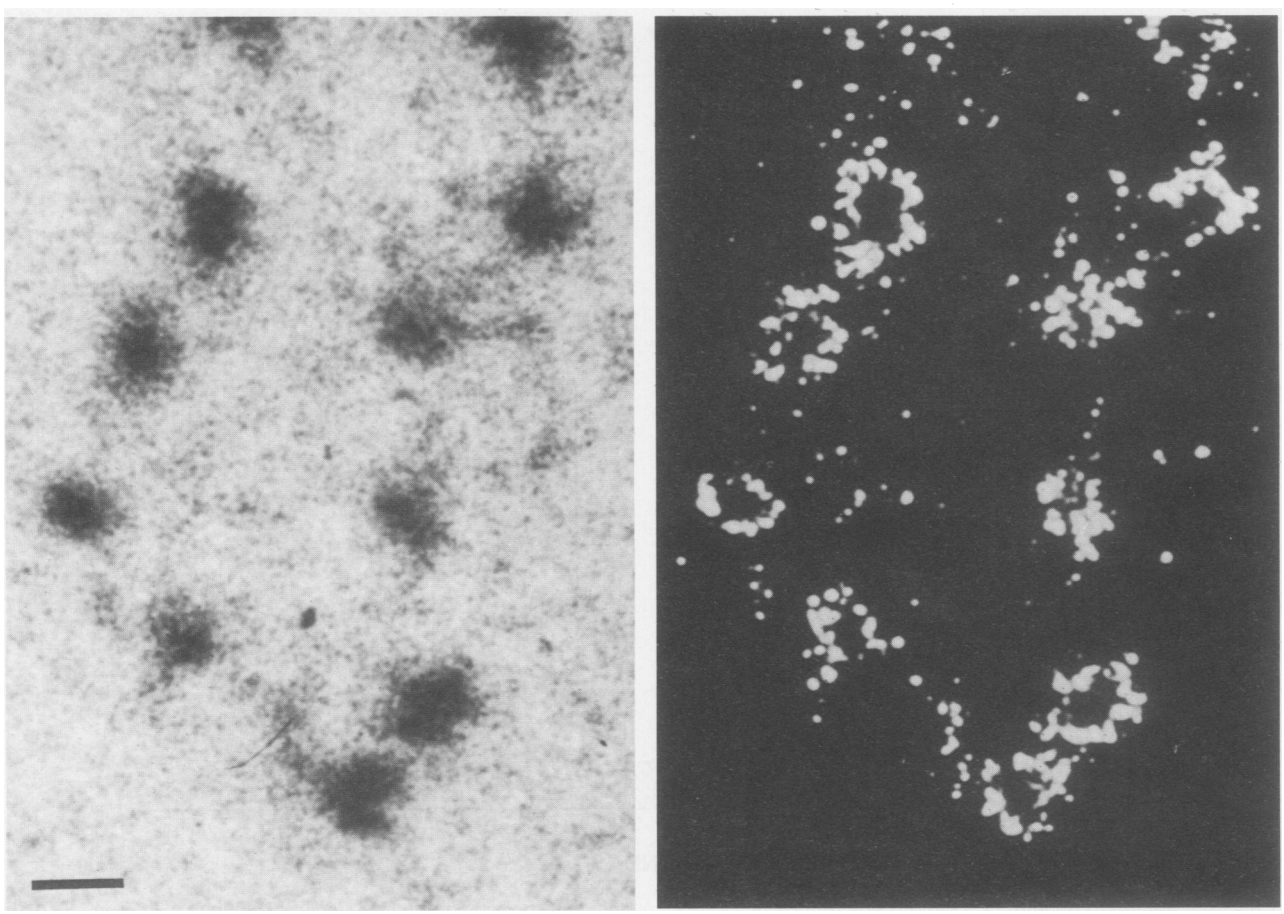

FIG. 5. ESI of nucleosomes prepared from calf thymus tissue. The reference image (110 eV) is on the left, and the net phosphorus image is on the right. Bar, 10 nm.

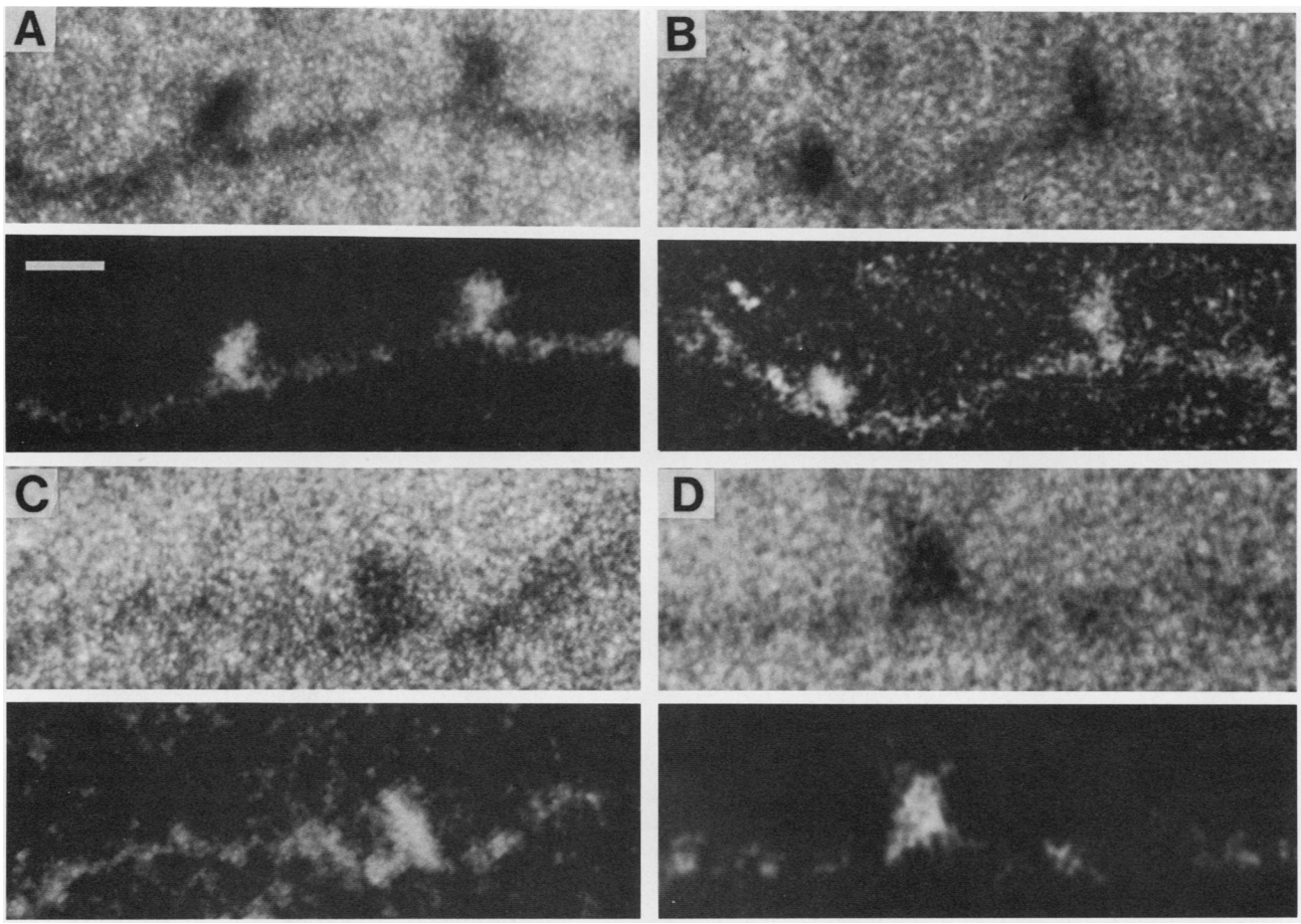

FIG. 6. ESI of complexes of TFIIIA with 5S RNA gene DNA. The complexes in panels A and B are on the plasmid pXlo8, and those in panels C and D are on the plasmid pXP-10. Reference images were recorded at 120 eV and are shown above the net phosphorus images of the same regions. These were obtained by the subtraction of the reference image from a phosphorus-enhanced image, recorded at 180 eV of energy loss. Bar, 10 nm.

Phosphorus analysis of TFIIIA-DNA complexes. ESI has provided two-dimensional maps of the phosphorus distribution and thus the DNA location in nucleoprotein complexes (1a). A reference image of nucleosomes prepared from calf thymus is shown (Fig. 5, left) along with the phosphorus distribution (Fig. 5, right). The ring appearance of the phosphorus content in the majority of the nucleosomes clearly indicates that the phosphorus is on the periphery of the particles. The fewer examples in the field where this ring pattern is not evident may represent particles whose supercoil axis is not oriented orthogonally to the support film.

Net phosphorus images of TFIIIA-DNA complexes were obtained to determine the spatial relationship between the protein and the DNA. Phosphorus distributions of six complexes are shown in the lower portion of the images (white on black) in Fig. 6 a to d. Surprisingly, the mass in each image that extends out from the flanking DNA helix contains phosphorus and the flanking DNA appears to enter and exit the complex at one end. Because of the compactness of the complex, we could not determine the location of the protein as we did in the nucleosome. The net phosphorus content of the complexes was calculated from the integrated signal over the area bounded by the complex and compared with the integrated signal along a known length of adjacent bare DNA, which served as an internal standard for a known number of phosphorus atoms. The average number of phosphorus atoms (30 complexes) was 119.2 ± 13.0, with a range from 68 to 186 (Fig. 7a). Some of the variation in the measurements may arise from the subjective determination of the boundaries of the complex, particularly at the base of the complex where the DNA enters and exists from the complex.

Since there are approximately 60 bp of DNA in the complex which appear in the phosphorus maps to extend approximately 9.5 nm out from the flanking DNA, we propose that the helix axis is distorted into a hairpin-shaped configuration, with 28 to 30 bp in both domains. The content of approximately 60 bp of DNA in the complex is also consistent with the attempt to determine their location by contour mapping. The correlation, within the error of measurement, between the mapped sites and known binding locations on the multiple-copy plasmid (pXlo8) was improved with the assumption that 50 to 60 bp of DNA was present in the complexes (data not shown).

We ruled out the possibility that a phosphorus signal could be generated by TFIIIA because of a putative phosphorylation of the protein or because of contaminating RNA fragments. This was accomplished by measuring the net phosphorus signal from purified TFIIIA by ESI. The average signal-to-noise ratio in the net phosphorus images over 29

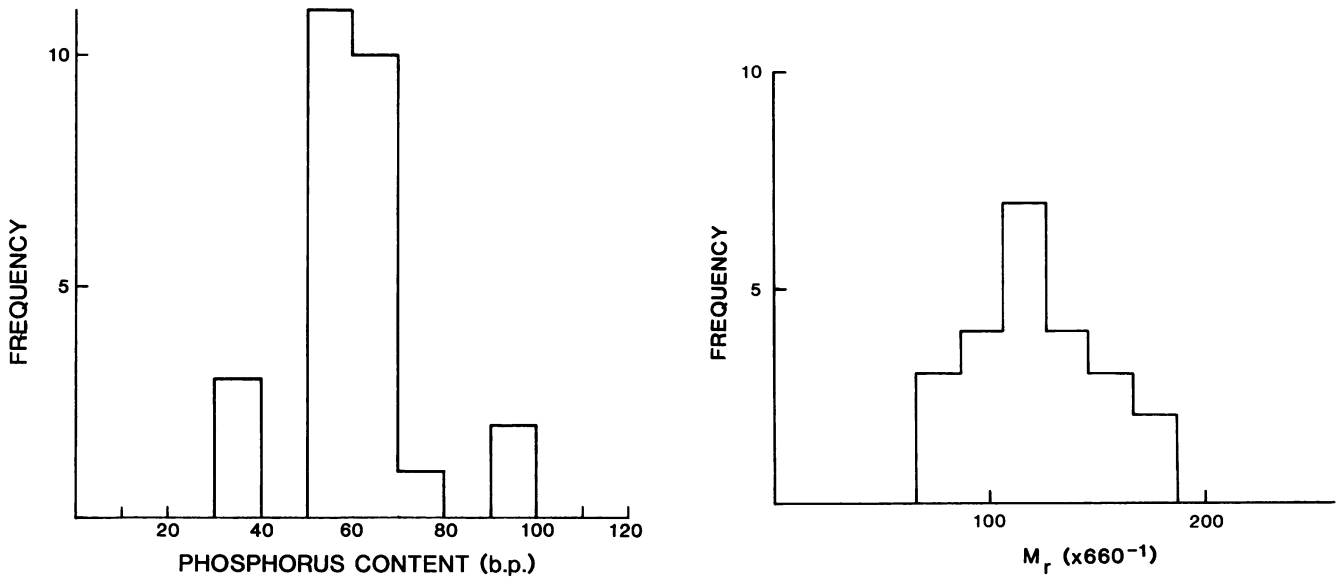

FIG. 7. (a) Histogram of electron spectroscopic measurements of phosphorus content of putative TFIIIA-DNA complexes expressed in base pairs of DNA. (b) Histogram of electron spectroscopic measurements of M_rs of putative TFIIIA-DNA complexes expressed in base pairs of DNA.

molecules was -0.7 ± 2.5, ranging from -5.0 to $+4.2$. A statistically significant phosphorus signal requires a signal-to-noise ratio of at least $+5$. The signal-to-noise ratio of the phosphorus signal for DNA was 14.

A measurement of the mass of the TFIIIA-DNA complex together with that of the phosphorus content gives the absolute content of both protein and nucleic acid. We used ESI to determine the mass of 30 complexes. The integrated optical density of the area represented by the complex was related to the integrated optical density of a length of flanking DNA, which was used as the known standard. For 30 complexes, the average mass (expressed in base pairs) was 124.5 ± 23.7, with a range from 84 to 189 (Fig. 7b). From these measurements the protein mass is the equivalent of 65 bp or 43,000 MW. The difference between this value and 39,000 MW, the known MW of TFIIIA, is well within the experimental error and therefore confirms that on average, only one molecule of TFIIIA binds to the internal control region (15).

Although the ability of TFIIIA to distort the DNA double helix has not been addressed, previous biochemical studies do not rule out this possibility. It is unlikely that the DNA is folded around the protein core, creating a supercoil as in the nucleosome. Biochemical evidence rules this out, since the binding of TFIIIA to closed plasmids causes only a slight amount of unwinding of the DNA double helix, an insufficient amount to account for a complete supercoil (10). Nevertheless, the nucleosome provides a clear precedent for the ability of proteins to bend DNA severely. Additionally, electron micrographs of transcription complexes involving factors and polymerase II also show that DNA can be bent by interactions with protein (16). The ability of the heat shock transcription factor to induce a bend in the DNA has also been demonstrated (14). It will be important to determine whether the ability to distort the DNA helix, as TFIIIA appears to do, is a general property of such regulatory factors.

We thank J. D. McGhee and J. M. Gottesfeld for helpful discussions and for reviewing the manuscript. We also thank D. D. Brown for the gift of the plasmids pXP-10 and pXlo8.

This work was supported by a grant from the Medical Research Council of Canada.

LITERATURE CITED

1. **Bazett-Jones, D. P.** 1988. Phosphorus imaging of the 7-S ribonucleoprotein particle. J. Ultrastruct. Mol. Struct. Res. **99**:59–69.
1a. **Bazett-Jones, D. P., L. Locklear, and J. B. Rattner.** 1988. Electron spectroscopic imaging of DNA. J. Ultrastruct. Mol. Struct. Res. **99**:48–58.
1b. **Brown, D. D., and J. B. Gurdon.** 1978. Cloned single repeating units of 5S DNA direct accurate transcription of 5S RNA when injected into Xenopus oocytes. Proc. Natl. Acad. Sci. USA **75**: 2849–2853.
2. **Engelke, D. R., S.-Y. Ng, B. S. Shastry, and R. G. Roeder.** 1980. Specific interaction of a purified transcription factor with an internal control region of 5S RNA genes. Cell **19**:717–725.
3. **Fairall, R., and A. D. Klug.** 1986. Mapping of the sites of protection on a 5S RNA gene by the Xenopus transcription factor IIIA. J. Mol. Biol. **192**:577–591.
4. **Gottesfeld, J. M.** 1987. DNA sequence-directed nucleosome reconstitution on 5S RNA genes of *Xenopus laevis*. Mol. Cell. Biol. **7**:1612–1622.
5. **Hanas, J. S., D. F. Bogenhagen, and C.-W. Wu.** 1983. Cooperative model for the binding of Xenopus transcription factor A to the 5S RNA gene. Proc. Natl. Acad. Sci. USA **80**:2142–2143.
6. **Lassar, A. B., P. L. Martin, and R. G. Roeder.** 1983. Transcription of class III genes: formation of preinitiation complexes. Science **222**:740–748.
7. **Miller, J., A. D. McLachlan, and A. Klug.** 1985. Repetitive zinc-binding domains in the protein transcription factor IIIA from Xenopus oocytes. EMBO J. **4**:1609–1614.
8. **Pelham, H. R. B., and D. D. Brown.** 1980. A specific transcription factor that can bind either the 5S RNA gene or 5S RNA. Proc. Natl. Acad. Sci. USA **77**:4170–4174.
9. **Picard, B., and M. Wegnez.** 1979. Isolation of a 7S-particle from Xenopus laevis oocyte: a 5S RNA protein complex. Proc. Natl. Acad. Sci. USA **76**:241–245.
10. **Reynolds, W. F., and J. M. Gottesfeld.** 1983. 5S gene transcription factor IIIA alters the helical configuration of DNA. Proc. Natl. Acad. Sci. USA **80**:1862–1866.
11. **Rhodes, D.** 1985. Structural analysis of a triple complex between the histone octamer, a Xenopus gene for 5S RNA and transcrip-

tion factor IIIA. EMBO J. **4**:3473–3482.
12. **Sakonju, S., D. F. Bogenhagen, and D. D. Brown.** 1980. A control region in the center of the 5S RNA gene directs specific initiation of transcription. I. The 5′ border of the region. Cell **19**:13–25.
13. **Shastry, B. S., S.-Y. Ng, and R. G. Roeder.** 1982. Multiple factors involved in the transcription of class III genes in Xenopus laevis. J. Biol. Chem. **257**:12979–12986.
14. **Shuey, D. J., and C. S. Parker.** 1986. Bending of promoter DNA on binding of heat shock transcription factor. Nature (London) **323**:459–461.
15. **Smith, D. R., I. J. Jackson, and D. D. Brown.** 1984. Domains of the positive transcription factor specific for the Xenopus 5S RNA gene. Cell **37**:645–652.
16. **ten Heggeler, B., and W. Wahli.** 1985. Visualization of RNA polymerase II ternary transcription complexes formed in vitro on a Xenopus laevis vitellogenin gene. EMBO J. **4**:2269–2273.
17. **Wolffe, A. P., E. Jordan, and D. D. Brown.** 1986. A bacteriophage RNA polymerase transcribed through a Xenopus 5S RNA gene transcription complex without disrupting it. Cell **44**:381–389.